PHYSICAL REVIEW B **78**, 081305(R) (2008)

Dynamics of the localized spins interacting with two-dimensional electron gas: Coexistence of mixed and pure modes

M. Vladimirova, S. Cronenberger, P. Barate, and D. Scalbert
Groupe d'Etude des Semi-conducteurs, UMR 5650, CNRS, Université Montpellier 2, Place Eugène Bataillon, Montpellier Cedex 34095, France

F. J. Teran
Departamento de Física de Materiales, Universidad Autònoma de Madrid, Madrid, 28049 Spain

A. P. Dmitriev
A. F. Ioffe Institute, 26 Polytechnicheskaya, St-Petersburg 194026, Russia
and Groupe d'Etude des Semi-conducteurs, UMR 5650, CNRS, Université Montpellier 2, Place Eugène Bataillon, Montpellier Cedex 34095, France

(Received 9 July 2008; revised manuscript received 24 July 2008; published 25 August 2008)

Time-resolved Kerr rotation experiments show that two kinds of spin modes exist in diluted magnetic semiconductor quantum wells: (i) strongly coupled electron-magnetic ion spin excitations and (ii) excitations of magnetic ion spin subsystem decoupled from electron spins. The coexistence of these two kinds of spin precession modes cannot be understood in terms of average spins but requires a description, which goes beyond the mean-field approximation.

DOI: 10.1103/PhysRevB.78.081305 PACS number(s): 75.50.Pp, 73.21.−b, 78.47.J−

Exchange interaction between spins is responsible for the collective nature of spin excitations in many solid-state systems. A good example is given by spin waves in ferromagnetic and antiferromagnetic materials.[1] In diluted magnetic semiconductors, the exchange interaction couples the itinerant carrier spins with the spins of magnetic impurities, e. g., Mn. Usually, the spin splitting of the carriers due to exchange interaction is much larger than Mn Zeeman splitting. However, at very low Mn concentrations (about 0.2%), resonant conditions can be achieved so that the frequency ω_e of the electron spin precession is close to the Mn spin precession frequency ω_m. In this case the exchange interaction may lead to the anticrossing of the spin precession frequencies. In *n*-doped CdMnTe quantum wells, the evidence of the strong-coupling regime has been provided.[2] It results in the formation of two mixed electron-ion spin modes. They are conveniently described within the mean-field approximation and correspond to the collective precession of the average electron and ion spins either with the same or with opposite phases [Figs. 1(a) and 1(b)]. Their frequencies $\omega_\pm$ are those of the two coupled oscillators,

$$\omega_\pm = \frac{1}{2}(\omega_e + \omega_m) \pm \frac{1}{2}\sqrt{(\omega_e - \omega_m)^2 + 4(\delta/\hbar)^2}, \qquad (1)$$

where δ is the interaction energy [Fig. 1(d)]. It was shown that δ is proportional to the electron gas spin-polarization degree.[3] Therefore, measuring resonant splitting between the collective modes provides valuable information on the spin-susceptibility enhancement in the two-dimensional electron gas.[4]

In this Rapid Communication we report on the coexistence of these strongly coupled electron—Mn spin modes and pure Mn spin excitations *decoupled* from the electron gas. The decoupled modes appear in the gap between the collective modes [Fig. 1(d)]. The existence of such decoupled Mn modes contradicts the commonly assumed mean-field physical picture and is not predicted by the recently developed many-body quantum theory of spin excitations in diluted magnetic semiconductors.[3,5]

We explain the ensemble of the spin modes in the framework of semiclassical model taking into account individual precession of *N* spins of Mn ions. Indeed, among *N* possible Mn spin precession modes, only one mode—where all the Mn spins precess with the same phase—couples strongly to the electron spins. This results in the formation of mixed *e*-Mn modes described by Eq. (1). In contrast, other $N-1$ Mn

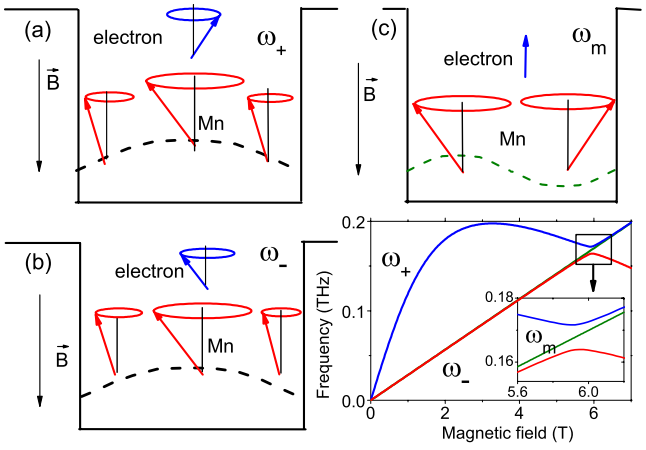

FIG. 1. (Color online) (a) and (b) Schematic representation of the mean-field collective spin precession modes and (c) the decoupled mode in CdMnTe quantum well. Dashed lines map spatial profile of the transverse spin component for the magnetic ions. Arrows are the snapshots of the precessing spin vectors of magnetic ions (long arrows) and electron (short arrows). (d) Field dependence of the mode frequencies $\omega_\pm$ and ω_m in the resonance region.

spin precession modes are characterized by zero average spin and, therefore, they remain pure Mn spin modes decoupled from the electron spin. The simplest case of a decoupled mode is illustrated in Fig. 1(c); two Mn spins placed symmetrically with respect to the well center precess with opposite phases, while the electron spin remains at equilibrium. Thus, coupling with the electron spin lifts the degeneracy of the Mn spin excitation spectrum and allows for the observation of the strongly coupled collective modes and pure Mn spin precession modes decoupled from the electron gas.

The samples that we study are two *n*-doped CdMnTe quantum wells with the concentration of magnetic ions $x=0.002$ (corresponding to a sheet density $n_m=2.4\times10^{13}$ cm^{-2}).[6] Electron concentrations are $n_e=0.7\times10^{11}$ cm^{-2} (sample 1) and $n_e=2.2\times10^{11}$ cm^{-2} (sample 2). This corresponds to zero-field Fermi energies $E_F=1.7$ and 5.3 meV for the samples 1 and 2, respectively. The well width is $w=100$ Å. The samples are placed in the cryostat at $T=2$ K under magnetic field $B\sim6$ T in the plane of the sample (along z axis).

The spin excitations are identified using all-optical spin-resonance technique.[7] The laser pulses of ~1.5 ps are tuned to the heavy-hole exciton transition at 764 nm and split into pump (200 μW) and probe (100 μW) pulses. Both beams are focused on the 200-μm-diameter spot on the surface of the sample. The pump-induced rotation of the linear polarization of the reflected probe (Kerr rotation) is measured as a function of delay between pump and probe pulses. Kerr rotation angle is proportional to the projection on the direction of the light of the total spin polarization created by the pump.

Prior to the excitation the magnetic ions and electrons are strongly spin polarized in the z direction. A circularly polarized pump pulse creates, in the quantum well, about 10^{10} cm^{-2} electrons and holes in the ground state. Their spins are polarized normal to the plane. This provides the initial fast rise of the signal. Because the heavy-hole g factor is vanishing in the direction perpendicular to the quantum-well axis, the hole spin does not precess. Its direct contribution to the Kerr signal decays during a short time $\tau_h\sim5$ ps and will not be important in the following. But the effective magnetic field created by the holes coherently rotates the spins of the magnetic ions away from the z direction.[8] This initiates the precession of the Mn spins around the total magnetic field created by the carriers and the external field. The electron spin is also expected to precess around the field created by the Mn spins and the external field.

Figure 2 shows the Kerr rotation signal measured at $B=6$ T, close to $\omega_e=\omega_m$, for the sample 1 [Fig. 2(a)] and the corresponding Fourier spectrum [Fig. 2(b)].[9] One can see that this signal contains *three* components. Two of them have similar amplitudes and relaxation times of about 30 ps but slightly different frequencies. These are the collective spin precession modes discussed in Refs. 2 and 3; their frequencies $\omega_\pm$ are given by Eq. (1). The third mode is related to the Mn spin excitations decoupled from the electron gas. Although about 15 times weaker than the collective modes, the third mode is unambiguously identified at resonance magnetic field ($B=6$ T) because it decays 60 times slower than the collective modes.

Figure 3(a) shows the precession frequencies measured as

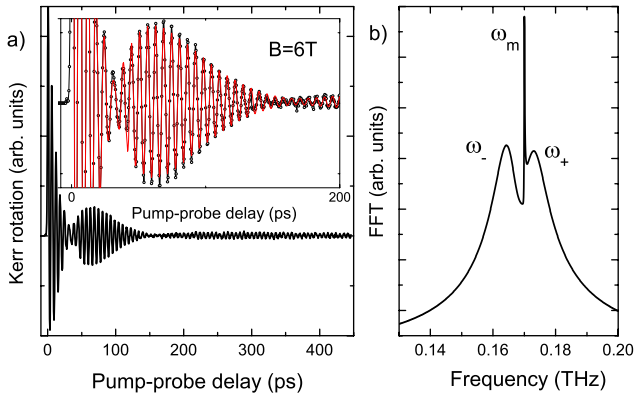

FIG. 2. (Color online) Time-resolved Kerr rotation at $B=6$ T for (a) the sample 1 and (b) the corresponding Fourier spectrum (Ref. 9). Inset: Zoom on the first 200 ps. Points show the data and the line is the fit with three damped cosines.

a function of the magnetic field. At low fields the electron-type mode frequency ω_+ is mainly determined by the Mn spin polarization J_z, which is described by the Brillouin function for the Mn spin value $J=5/2$. At higher fields the magnetization saturates, ω_+ reaches its maximum, and then decreases due to Zeeman effect. The fraction of the magnetic impurities $x=0.002$ and the Mn spin temperature $T_{\mathrm{Mn}}=3.8$ K can be accurately determined from this dependence. The frequency ω_- of the Mn-type mode increases linearly with the field and the resonance $\omega_e=\omega_m$ is reached near $B=6$ T. The resonance region is plotted in details in Fig. 3(b) (frequencies) and Fig. 3(c) (decay times). One can see a clear anticrossing of the two modes $\omega_\pm$ and a rapid variation of their decay times. Indeed at $B=5.7$ T the decay times of Mn-type and electron-type modes differ by an order of magnitude; at resonance field $B\sim6$ T the corresponding decay times become equal. This behavior is easily understood in terms of two coupled modes with very different dampings.

The third mode frequency emerges in the gap between the two collective modes (Fig. 3). Its field dependence (tri-

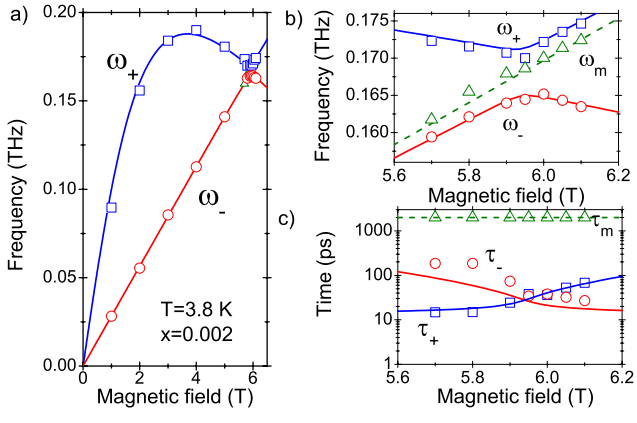

FIG. 3. (Color online) (a) Spin precession frequencies and (b) decay times extracted from Kerr rotation measurements under magnetic field $B=5.7-6.1$ T (sample 1). Symbols show the experimental data and solid lines are the best fit obtained for the collective modes using Eqs. (1) and (8). Dashed lines show Mn spin excitations decoupled from electrons.

angles) is linear and is given by Mn g factor $g_m=2.02$.[10,11] It has the longest relaxation time, which exceeds the accessible delays in our setup, but estimated to be about 2 ns. Thus, some excitations of the magnetic ion spins appear to be decoupled from the electrons.

In order to explain the origin of the decoupled Mn spin mode, we must remember that Mn spin dynamics is not fully reduced to the precession of the average spin, in contrast to usual assumption. We develop a simple model where the individual Mn spins may precess with different phases. The assumptions of the model are listed below. First of all, we consider spin excitations, which are homogeneous in the plane of the sample, so that the spins of the ions lying in the same crystallographic plane are identical. For simplicity, the distribution of Mn ions across the sample is supposed to be homogeneous. Following other authors,[3,12] we neglect the effect of the random impurity potential on the electron wave functions and limit the consideration to the lowest quantization level in the quantum well. The corresponding electron wave function is $\phi(x,\mathbf{r})=\chi(x)\exp(i\mathbf{kr})/\sqrt{A}$, where $\chi(x)$ is the electron wave function in the quantization direction, A is the sample area, and $\mathbf{k}$ and $\mathbf{r}$ are wave vector and coordinate of the electron in the plane of the structure, respectively.

Under these conditions the dynamics of the average electron spin $\mathbf{S}$ and the spins of the magnetic ions $\mathbf{J_k}$ is given by the system of the Bloch equations,

$$\frac{d\mathbf{S}}{dt}=-\frac{g_e\mu_B}{\hbar}(\mathbf{S}\times\mathbf{B})+\frac{\alpha}{\hbar}\sum_k|\phi(\mathbf{R_k})|^2(\mathbf{S}\times\mathbf{J_k}), \tag{2}$$

$$\frac{d\mathbf{J_k}}{dt}=-\frac{g_m\mu_B}{\hbar}(\mathbf{J_k}\times\mathbf{B})-\frac{\alpha n_e\chi^2(\mathbf{R}_k)}{\hbar}(\mathbf{S}\times\mathbf{J_k}). \tag{3}$$

Here $g_e=-1.5$ is the electron g factor[13] and μ_B is the Bohr magneton. The last terms in Eqs. (2) and (3) account for the exchange interaction of the ferromagnetic type between the electrons and Mn spins ($\alpha=1.5\times10^{-23}$ eV/cm^3). Vectors $\mathbf{R}_k$ denote the positions of the ions.

The experimentally detected nonequilibrium transverse spin components are small with respect to the equilibrium spin values $\mathbf{S_z}$ and $\mathbf{J_z}$. Therefore, Eqs. (2) and (3) can be linearized. Taking into account the in-plane homogeneity of the problem, we can limit the number of Eq. (3) to the number of crystallographic planes in the quantum well. Then, for the nonequilibrium (transverse) spin components of the electron $\mathbf{S}_\perp$ and the ions $\mathbf{J}_{\perp,\mathbf{n}}$, the linearized Bloch equations read

$$\frac{d\mathbf{S}_\perp}{dt}=-(\mathbf{S}_\perp\times\mathbf{\Omega_e})+\frac{\Delta}{J_z}(\mathbf{J}_\perp\times\mathbf{S_z}), \tag{4}$$

$$\frac{d\mathbf{J}_{\perp,\mathbf{n}}}{dt}=-(\mathbf{J}_{\perp,\mathbf{n}}\times\mathbf{\Omega_m})-\frac{K}{S_z}w\chi_n^2(\mathbf{J}_{\perp,\mathbf{n}}\times\mathbf{S_z})+\frac{K}{S_z}w\chi_n^2(\mathbf{S}_\perp\times\mathbf{J_z}), \tag{5}$$

where χ_n denotes the value of $\chi(x)$ in the nth crystallographic plane. $\mathbf{J}_\perp\equiv(w/N)\Sigma_{n=1}^N\chi_n^2\mathbf{J}_{\perp,\mathbf{n}}$ is the average spin of the ions—weighted by the probability to find an electron in the nth layer. The first term in the right-hand part of Eq. (4) describes the precession of the transverse component of the electron spin in an effective field. This field is a combination of the external field $\mathbf{B}$ and exchange field created by the equilibrium component of the ion spins. The precession frequency is given by $\mathbf{\Omega_e}=g_e\mu_B\mathbf{B}/\hbar+\Delta\mathbf{J_z}/J_z$, with $\Delta=-\alpha n_m J_z/\hbar w$. In Eq. (5), the first two terms are the precession of the transverse component of the Mn spins in the external field with the frequency $\mathbf{\Omega_m}=g_m\mu_B\mathbf{B}/\hbar$ and in the weak exchange field created by the electrons and proportional to $K=-\alpha n_e S_z/w\hbar\ll\Delta$. The last terms in Eqs. (4) and (5) describe the interaction between nonequilibrium components of electron and ion spins.

The above equations describe the system of coupled oscillators and can be solved exactly.[14] However, it is instructive to make an additional approximation and neglect the precession of Mn spins in the static exchange field created by the electrons. This is justified since this field is about 1000 times weaker than the external field. Thus, Eq. (5) becomes

$$\frac{d\mathbf{J}_{\perp,\mathbf{n}}}{dt}=-(\mathbf{J}_{\perp,\mathbf{n}}\times\mathbf{\Omega_m})+\frac{K}{S_z}w\chi_n^2(\mathbf{S}_\perp\times\mathbf{J_z}). \tag{6}$$

Equations (4) and (6) describe $N+1$ modes. Two of these modes correspond to the collective motion of spins $\mathbf{J}_\perp$ and $\mathbf{S}_\perp$ with the frequencies $\omega_\pm$ given by Eq. (1) with $\omega_e=\Omega_e$, $\omega_m=\Omega_m$, $\delta^2=\eta K\Delta$, and $\eta=w\int_0^w\chi^4(x)dx$.[15] These are the collective modes discussed in Refs. 2 and 3. The other $N-1$ modes satisfy the conditions

$$\mathbf{J}_\perp\equiv(w/N)\sum_{n=1}^N\chi_n^2\mathbf{J}_{\perp,\mathbf{n}}=0,\quad \mathbf{S}_\perp=0. \tag{7}$$

They are degenerate and correspond to the Mn spin precession at frequency Ω_m. In each of the $N-1$ mode, the distribution of the transverse Mn spin components across the quantum well $\mathbf{J}_{\perp,\mathbf{n}}$ is orthogonal to the distribution of electron density χ_n^2. Therefore, the total exchange field that they create on electrons is zero and average electron spin does not precess. Thus, an arbitrary spin excitation is a combination of two mean-field collective modes with eigenfrequencies $\omega_\pm$ and $N-1$ pure modes where magnetic ions precess at frequency Ω_m. It should be noted that in asymmetric quantum wells, the pure modes can be optically excited and detected via valence-band states because the symmetry of the hole wave function is different from the electron one in such structures.

Let us now address the relaxation of these modes. The relaxation of the decoupled modes is hidden in the small term that we neglected in the right part of the Eq. (5). Solving the full system of Eqs. (4) and (5) one can see that it is responsible for the lifting of the degeneracy of the $N-1$ decoupled modes and, thus, leads to the broadening of the corresponding spin resonance $\delta\omega\sim K$. The corresponding dephasing time yields $\tau_m\sim1/K$. In contrast, the collective modes do not decay in the framework of the above model because the rapid relaxation of the electron spin was omitted. Therefore, electron spin relaxation should be taken into account. This can be done phenomenologically by introducing in the right part of Eq. (4) an additional term $-\mathbf{S}_\perp/\tau_e$, where

τ_e is the electron spin relaxation time far from resonance. This term affects neither the frequencies nor the damping of the decoupled modes. The two collective modes $\omega_\pm$ are again given by Eq. (1) with

$$\omega_e = \Omega_e + i/\tau_e, \quad \omega_m = \Omega_m. \tag{8}$$

Their relaxation times result from the imaginary part of the complex frequencies and at resonance are both equal to $2\tau_e$. The gap between the collective modes is reduced by the electron spin relaxation so that $2\delta = 2\sqrt{\eta K\Delta - (1/2\tau_e)^2}$.

The predictions of our simple model meet perfectly the experimental results. For the collective modes, frequencies and decay times calculated using Eqs. (1) and (8) are shown in Fig. 3 by solid lines. The spin-polarization degree of the electron gas ($P=50\%$ in sample 1), which determines the value of $K=0.34$ μeV, is the only fitting parameter in this calculation. The electron spin decay time out of resonance $\tau_e=15$ ps, as well as the electron exchange splitting $\Delta=1.2$ meV as a function of the magnetic field, are directly extracted from the Kerr rotation measurements. At resonance we get the splitting between the collective modes $2\delta=30$ μeV. The anticrossing energy appears to be substantially reduced by the electron spin resonance broadening neglected in the previous works.[2,3] Note also that the values of τ_e measured far from resonance are substantially shorter than the theoretical predictions $\tau_e \approx 100$ ps.[12] We suggest that it is mainly due to electron spin dephasing governed by the fluctuations of the exchange field created by the ions. The determination of the characteristic length scale at which the electrons probe these fluctuations is beyond the scope of this work and requires further theoretical work. For the decoupled modes the estimation of the dephasing time using $\tau_m \sim 1/K$ gives about 1 ns. This is consistent with the experimental data [dashed line in Fig. 3(c)], while it is much shorter than any homogeneous relaxation time.[16]

For the sample 2 we measure $\Delta=1.2$ meV, $\tau_e=20$ ps, $2\delta=20$ μeV, and $\tau_m \sim 1$ ns, which yields $K=0.2$ μeV and $P=10\%$. In both samples the spin polarization of electron gas is enhanced with respect to that of noninteracting electrons [$P=25\%$ (7%) in the sample 1 (2)].[4] Thus, measuring the spin excitation spectrum in diluted magnetic quantum wells appears to be an excellent tool to explore the fundamental properties of spin-polarized electron gas.

In conclusion, we have shown that in the system of localized spins interacting with the two-dimensional electron gas, strongly coupled collective spin excitations coexist with the excitations of the localized spins, which are decoupled from the electron spin. This experimental fact cannot be explained in the mean-field approximation. We interpret the ensemble of our experimental observations in the framework of the simple semiclassical model taking into account the precession of the localized spins individually.

We acknowledge the helpful discussions with M. I. Dyakonov and the support from the ANR project "GOSPININFO." A.P.D. acknowledges the support from RFBR, Russian Scientific School, and programs of RAS.

[1] Ch. Kittel, *Quantum Theory of Solids* (Wiley, New York, 1987).
[2] F. J. Teran, M. Potemski, D. K. Maude, D. Plantier, A. K. Hassan, A. Sachrajda, Z. Wilamowski, J. Jaroszynski, T. Wojtowicz, and G. Karczewski, Phys. Rev. Lett. **91**, 077201 (2003).
[3] J. König and A. H. MacDonald, Phys. Rev. Lett. **91**, 077202 (2003).
[4] F. Perez, C. Aku-leh, D. Richards, B. Jusserand, L. C. Smith, D. Wolverson, and G. Karczewski, Phys. Rev. Lett. **99**, 026403 (2007).
[5] D. Frustaglia, J. König, and A. H. MacDonald, Phys. Rev. B **70**, 045205 (2004).
[6] V. Huard, R. T. Cox, K. Saminadayar, A. Arnoult, and S. Tatarenko, Phys. Rev. Lett. **84**, 187 (2000).
[7] J. M. Kikkawa and D. D. Awschalom, Science **287**, 473 (2000).
[8] C. Camilleri, F. Teppe, D. Scalbert, Y. G. Semenov, M. Nawrocki, M. Dyakonov, J. Cibert, S. Tatarenko, and T. Wojtowicz, Phys. Rev. B **64**, 085331 (2001).
[9] The results are very similar for the sample 2. The Fourier spectrum is obtained from the fit of the data.
[10] S. A. Crooker, D. D. Awschalom, J. J. Baumberg, F. Flack, and N. Samarth, Phys. Rev. B **56**, 7574 (1997).
[11] R. Akimoto, K. Ando, F. Sasaki, S. Kobayashi, and T. Tani, Phys. Rev. B **57**, 7208 (1998).
[12] Y. G. Semenov, Phys. Rev. B **67**, 115319 (2003).
[13] A. A. Sirenko, T. Ruf, M. Cardona, D. R. Yakovlev, W. Ossau, A. Waag, and G. Landwehr, Phys. Rev. B **56**, 2114 (1997).
[14] These equations can also be obtained by the minimization of the effective action calculated in Ref. 3, Eq. (8).
[15] In the approximation of the square well with infinite barriers, electron wavefuction reads $\chi(x)=(\sqrt{2/w})\sin(\pi x/w)$ and $\eta=3/2$. Note also that the factor η is absent in the expression for δ^2 from Ref. 3, were the role of $\mathbf{J}_\perp$ is played by the average spin of the ions.
[16] B. König, I. A. Merkulov, D. R. Yakovlev, W. Ossau, S. M. Ryabchenko, M. Kutrowski, T. Wojtowicz, G. Karczewski, and J. Kossut, Phys. Rev. B **61**, 16870 (2000).